CURRENT PROBLEMS IN RAIL VEHICLES

XXVII. conference with international participation
17–19 September 2025, Česká Třebová

EXPERIMENTAL PROOF OF SPIN INFLUENCE ON RAIL-WHEEL CONTACT FORCES: MEASUREMENTS DESIGN ON ROLLER TEST RIG

EXPERIMENTÁLNÍ OVĚŘENÍ VLIVU SPINU NA SÍLY V KONTAKTU KOLO–KOLEJNICE: NÁVRH MĚŘENÍ NA KLADKOVÉM STAVU

Jan PULDA[1], Petr VOLTR[2], Bohumil CULEK[3]

e-ISBN: 978-80-7560-564-1
DOI: 10.46585/spkv20252682
ISSN: 3029-8342

CC BY

Abstract

For assessment of an influence on contact forces distribution in rail-wheel contact a roller test rig is going to be used – Railway Wheel Test Rig (RWTR), which is located in the authors' workplace. RWTR approximates conditions in rail-wheel contact with contact geometry, magnitude of wheel forces, rotational velocity, angle of attack. For the designed experiments, an augmentation of the installed measuring system is required. This paper deals with an analysis of requirements for designed experiments of spin influence and with a complex revision of a current measuring system of all quantities on RWTR. From this analysis we conclude measurement modifications, mainly with respect to the rollers' relative position.

Keywords

rail-wheel contact, adhesion, spin creepage, roller test rig, measuring system

Abstrakt

Pro účely výzkumu vlivu spinu na rozložení sil v kontaktu kola s kolejnicí bude použit kladkový zkušební stav – Testovací zařízení železničních kol (TZŽK) – instalovaný na pracovišti autorů. Podmínkám v kontaktu kolo–kolejnice se TZŽK přibližuje kontaktními podmínkami, velikostmi kolových sil, rychlostmi rotace, nastavením úhlu náběhu. Pro navrhované experimenty je potřeba zpřesnit instalovaný měřicí systém. Tento příspěvek se zabývá rozborem požadavků na navrhované experimenty vlivu spinu a komplexní revizí současného měřicího systému všech veličin instalovaného na TZŽK. Z tohoto rozboru vyplývá návrh úprav měření, zejména s ohledem na měření vzájemné polohy kladek.

Klíčová slova

kontakt kolo–kolejnice, adheze, spinový skluz, kladkový zkušební stav, měřicí systém

[1] **Ing. Jan Pulda**, ORCID 0009-0008-4272-9381. University of Pardubice, Faculty of Transport Engineering, Department of Transport Means and Diagnostics. Studentská 95, 532 10 Pardubice, Czech Republic, e-mail: jan.pulda@student.upce.cz

[2] **doc. Ing. Petr Voltr, Ph.D.**, ORCID 0000-0001-7516-1069. University of Pardubice, Faculty of Transport Engineering, Educational and Research Centre in Transport. Studentská 95, 532 10 Pardubice, Czech Republic, phone: +420 466 038 505, e-mail: petr.voltr@upce.cz

[3] **prof. Ing. Bohumil Culek, CSc.**, ORCID 0000-0002-0098-9934. University of Pardubice, Faculty of Transport Engineering, Department of Transport Means and Diagnostics. Studentská 95, 532 10 Pardubice, Czech Republic, phone: +420 466 038 511, e-mail: bohumil.culek@upce.cz

1 INTRODUCTION

If two elastic bodies are pushed into contact with a force, they are in relative motion and friction occurs in this contact, traction forces (tangential to contacting surfaces) are generated. The generation of traction forces is described with the theory of adhesion. In principle, the relative motion causes deformations in the contacting surfaces, which in turn generate traction forces. Thus, the description of the relative motion between the bodies and its link to traction forces is crucial for the theory of adhesion. To describe kinematics, we use three relative quantities [1]:

- s_x – longitudinal creepage,
- s_y – lateral creepage,
- ϕ_z – spin creepage.

Spin creepage describes the relative rotational movement around the normal to the contact patch. According to theory and experiments, spin induces lateral creep force and moment around the normal [1]. For experimental analysis, measuring lateral creep force is the most convenient way to assess the influence of spin. The basis of this approach is the determination of lateral creep characteristics (i.e. relation between lateral creepage s_y and lateral creep force T_y) for a fixed value of spin. All possible approaches to the experimental analysis are thoroughly discussed in [2]. We can formally express the interconnections between quantities changeable during experiments on a roller test rig: creep forces, contact loading, and kinematics using equations (1) and (2). Creep forces also depend on other parameters, e.g. material properties and friction coefficient, which we consider constant for experiments.

$$T_{\mathrm{x}} = f(s_{\mathrm{x}}, s_{\mathrm{y}}, \phi_{\mathrm{z}}, N) \tag{1}$$

$$T_{\mathrm{y}} = f(s_{\mathrm{x}}, s_{\mathrm{y}}, \phi_{\mathrm{z}}, N) \tag{2}$$

Paper [2] states that the roller test rig (*Railway Wheel Test Rig – RWTR*; in Czech *Testovací zařízení železničních kol – TZŽK*) installed at the Educational and Research Centre in Transport, Faculty of Transport Engineering, University of Pardubice is suitable for experiments designed to investigate spin influence. Although RWTR was developed for experiments concerning rail-wheel contact forces (such as development of an instrumented wheelset [3]), there was initially no need to measure all required quantities with the desired precision (current state is described in Chapter 3). Thus, for the planned experiments of spin influence, the measuring system requires improvement.

2 THEORETICAL BACKGROUND

For the planned experiments, it is necessary to define the measurable quantities, the evaluation quantities, and the mathematical relations between them. In principle, we must determine the set of *principal quantities*, which are used for evaluating the experiment. However, these quantities are not directly measurable and must be derived from measured quantities. These quantities can then be divided into those describing kinematics and those describing forces. The relationships between the measured and principal quantities, as well as the measuring devices, are summarised in Tab. 1.

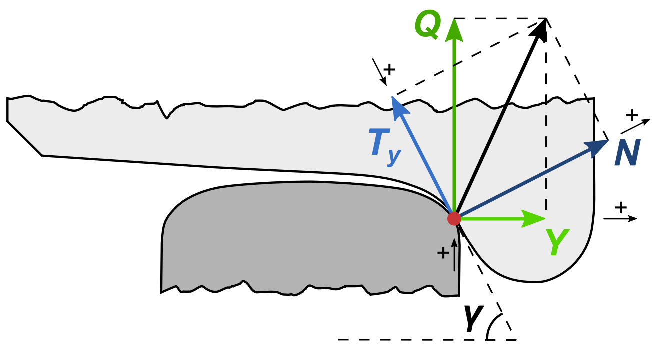

Fig. 1 Derivation of a force transformation in the contact

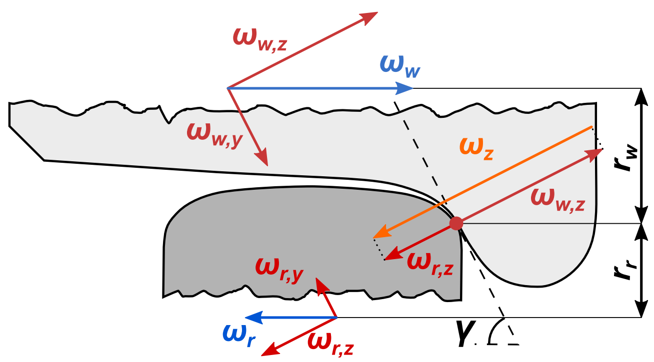

Fig. 2 Derivation of the spin creep angular velocity

Tab. 1 Summary of principal and measured quantities

Name	**Abbr.**	**Note – Measuring device**
Principal quantities – forces		
Normal force in contact	N	Not directly measurable (derived) Determined from Q, Y and contact geometry (see Eqn. (3))
Longitudinal creep force in contact	T_{x}	Not directly measurable (derived) Determined from M_T and contact geometry
Lateral creep force in contact	T_{y}	Not directly measurable (derived) Determined from Q, Y and contact geometry (see Eqn. (4))
Spin moment in contact	M_{z}	Not directly measurable (derived) Omitted due to presumed small magnitude
Principal quantities – kinematics		
Longitudinal creepage	s_{x}	Not directly measurable (derived) Determined from ω_{w}, ω_{r} and contact geometry (see Eqn. (6))
Lateral creepage	s_{y}	Not directly measurable (derived) Determined from α and contact geometry (see Eqn. (7))
Spin creepage	ϕ_{z}	Not directly measurable (derived) Determined from contact geometry (see Eqn. (8))
Measured quantities – forces		
Vertical wheel force	Q $[FQ]$	Instrumentation of the rail roller (strain gauges + calculation) [Reaction forces in wheel frame attachments (strain gauges) Reaction force in rail roller frame linear actuator (load cell)]
Lateral wheel force	Y $[FY]$	Instrumentation of the rail roller (strain gauges + calculation) [Reaction forces in wheel frame attachments (load cell)]
Traction moment on the rail roller	M_{T}	Instrumentation of the rail roller shaft (strain gauges)
Measured quantities – kinematics		
Lateral relative position of the rollers	y	Four-point laser measuring system (Chapter 4.1)
Angle of attack of the rollers	α	Four-point laser measuring system (Chapter 4.1)
Rail roller angular velocity	ω_{r}	Optical incremental encoder on a shaft
Wheel roller angular velocity	ω_{w}	Optical incremental encoder on a shaft
Roll angle deviation	ψ	Not directly measurable Determined from position of a wheel roller frame
Premeasured characteristics		
Contact geometry of the rail roller		Lateral profile + reference roller radius
Contact geometry of the wheel roller		Lateral profile + reference roller radius

The simplest case considers a planar contact patch with constant conditions (rolling radii r and contact patch angle γ). Eqns. (3) and (4) can be derived for the forces, based on the force transformation within the contact patch (see Fig. 1).

$$N = Q \cdot \cos\gamma + Y \cdot \sin\gamma \tag{3}$$

$$T_{\mathrm{y}} = -Q \cdot \sin\gamma + Y \cdot \cos\gamma \tag{4}$$

To calculate the creepages describing the kinematics, a reference velocity must be defined. For this purpose, we adopt the standard definition given in Eqn. (5) (see [1]).

$$v_{\mathrm{ref}} = -\frac{1}{2}|\omega_{\mathrm{r}} \cdot r_{\mathrm{r}} + \omega_{\mathrm{w}} \cdot r_{\mathrm{w}}| \tag{5}$$

Using this definition, the relative creepages can be calculated. They are based on the components of slip velocity $\boldsymbol{w}$ and the spin angular velocity ω_{z} (see [7] and principle of derivation in Fig. 2). These relations are given in Eqns. (6) – (8). The slip velocity and the spin angular velocity depend on the angular velocities ω of the rollers, the angle of attack α, and on the contact conditions – rolling radii r of the rollers and the contact patch angle γ. These latter quantities depend on a contact patch position and thus on the lateral relative position y of the rollers. Determination depends on contact search algorithm. For example, CONTACT software, used in numerical analysis (see Chapter 4), uses rigid body assumption with refinements [9]. More complex situation is for conformal contact. For this case, the contact conditions change significantly even within the contact patch [10]. Thus, its analysis is beyond the scope of this paper.

$$w_{\mathrm{x}} = \omega_{\mathrm{r}} \cdot r_{\mathrm{r}} - \omega_{\mathrm{w}} \cdot r_{\mathrm{w}} \Rightarrow s_{\mathrm{x}} = \frac{w_{\mathrm{x}}}{v_{\mathrm{ref}}} \tag{6}$$

$$w_{\mathrm{y}} = -\omega_{\mathrm{w}} \cdot r_{\mathrm{w}} \cdot \frac{\alpha}{\cos\gamma} \Rightarrow s_{\mathrm{y}} = \frac{w_{\mathrm{y}}}{v_{\mathrm{ref}}} \tag{7}$$

$$\omega_{\mathrm{z}} = (\omega_{\mathrm{r}} - \omega_{\mathrm{w}}) \cdot \sin\gamma \Rightarrow \phi_{\mathrm{z}} = \frac{\omega_{\mathrm{z}}}{v_{\mathrm{ref}}} = \left(\frac{1}{r_{\mathrm{r}}} + \frac{1}{r_{\mathrm{w}}}\right) \cdot \sin\gamma \tag{8}$$

3 DESCRIPTION OF THE CURRENT STATE OF THE ROLLER TEST RIG (RWTR)

This chapter describes the current state of the RWTR. The focus is on the mechanical design and the design of the measuring system. A detailed description of the current state is provided in [4], [5] and [6].

Mechanical Design

The RWTR consists of two rollers – a standard railway wheel and a rotating rail. A photo of RWTR is in Fig. 3 and its structure is illustrated schematically in Fig. 4. Each roller is driven by a fully controlled electric motor, allowing simulation of traction and braking. The rail roller is mounted in a frame that enables both longitudinal and lateral motion relative to the wheel roller. The angle of attack is set up on the frame of the wheel roller. All these motions are driven by electric linear actuators. The wheel roller has nominal diameter 920 mm and is equipped with standard S1002 profile, and the rail roller has nominal diameter 1245 mm and is equipped with S 49 profile with inclination 1:40. Therefore, the RWTR approximates rail–wheel contact conditions in terms of contact geometry, force magnitudes, and relative movements.

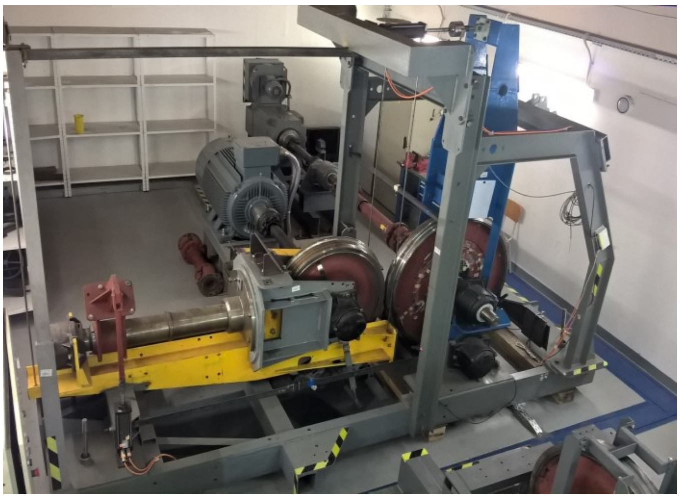

Fig. 3 Photo of RWTR

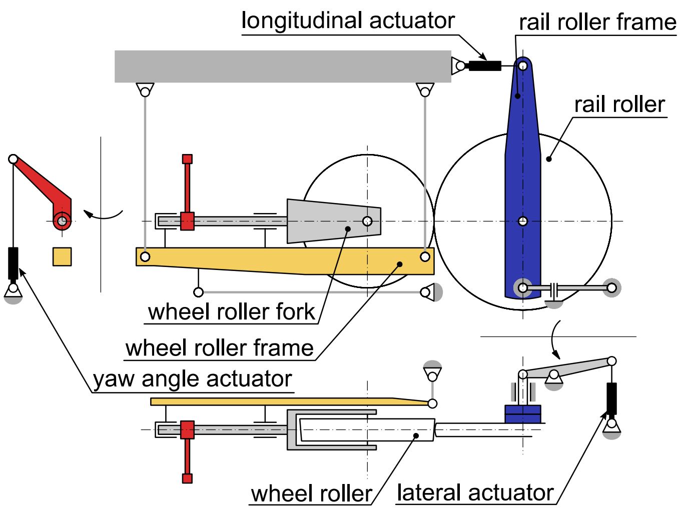

Fig. 4 Mechanical schematics of RWTR (without electric motors)

Measuring System

The measuring system is a standard electronic measuring system (EMS), which consists of the measuring chain: analogue sensor → A/D converter → recording computer. The current system topology and data flow are illustrated in Fig. 5. Current measuring points are shown in the schematics Fig. 6.

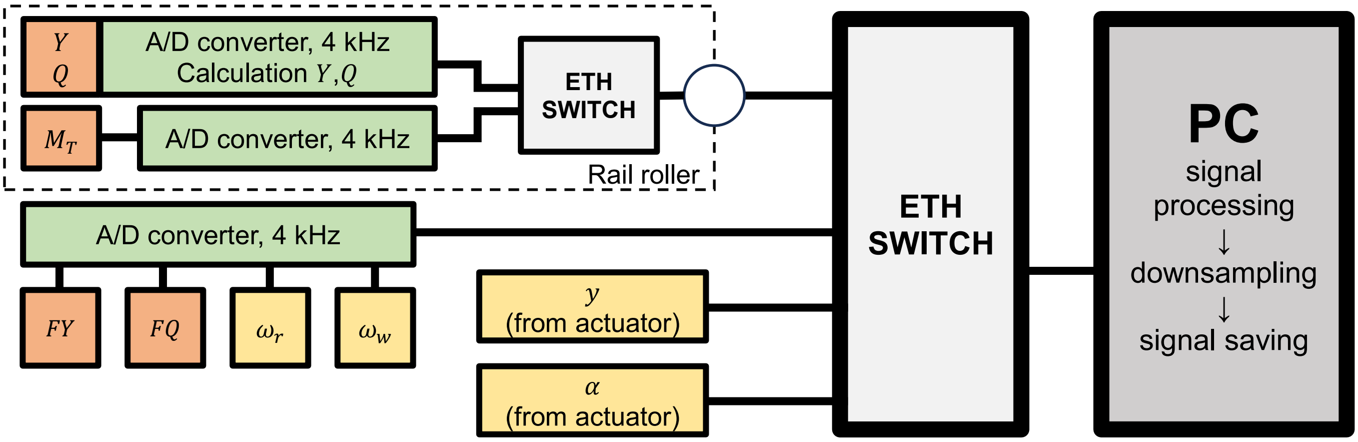

Fig. 5 Current topology of the measuring system installed on RWTR

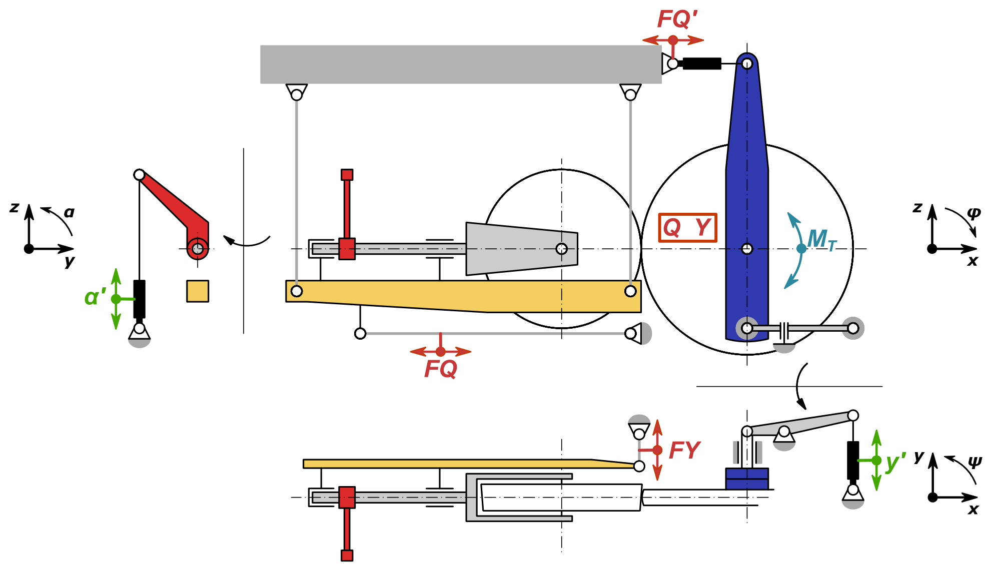

Fig. 6 Schematics of current points of measurements, abbreviations with prime (') mark recalculation of the measured value to actual value of the quantity (e.g. lever ratio)

4 DESIGN OF MEASUREMENTS

As stated in the Introduction, the measuring system described in Chapter 2 requires improvement. Firstly, an analysis is provided of which quantities are required for the evaluation of spin experiments (see Chapter 2). The measurements of forces and angular velocities are described in the references, and no significant changes are anticipated. On the other hand, the measurement of displacements requires substantial improvement; therefore, their design is discussed in detail in the following chapter.

4.1 Displacement Measurements

A crucial part of the planned experiments is the precise measurement of **the lateral position** between the rollers and **their angle of attack**. Due to the high sensitivity of the contact point position to the lateral alignment of the rollers (particularly during flanging), high precision of the measurement is required. Until now, these measurements have been taken indirectly using the measured displacements of the linear actuators. Therefore, these measurements were not precise enough (± 0.2 mm for each displacement [6]). This chapter proposes a new design of the measurement system.

Measurements Requirements

Tab. 2 provides an analysis of all possible movements (degrees of freedom – DoF) of the rollers. Some of these movements are required, while others are considered parasitic. Rotation around the z-axis (ψ) deserves special attention. According to [7], this parasitic movement can significantly affect the contact angle, thereby altering the spin magnitude (see Eqn. (8)). The proposed measurement system takes these movements into account.

Tab. 2 Overview of possible movements of the rollers

DoF	Rail roller		Wheel roller	
x	---	Moving together	---	Moving together
y	Required	Measured	Parasitic	Measured
z	---	Due to rigidity negligible	Parasitic	Influence on measurement negligible
α	Parasitic	Fully measured	Required	Fully measured
ϕ	Required	Own rotation	Required	Own rotation
ψ	---	Due to rigidity negligible	Parasitic	Measured

Another requirement arises from the contact conditions and precision of a contact region determination. This could be significant for significantly non-Hertzian geometry (e.g. changes in profile curvature on a rail head profile) or for profiles with steep changes in slope (e.g. transition to a flange of a wheel profile). To illustrate these effects, in Tab. 3 there are calculated values of guiding force Y for different contact conditions. The contact is in transition to a flange. From this point the lateral position of rollers and angle of attack is changed. The situation is also documented in Fig. 7 with gradual change of lateral position the rollers in flange transition.

To maintain the variation in the lateral force Y due to measurement uncertainty below 5 %, the uncertainty in lateral position must be within $0.01\ \mathrm{mm}$ and in angle of attack within $0.2\ \mathrm{mrad}$. **However, achieving such precision is not feasible.** Therefore, we also consider modifying the rollers' profiles to reduce the Y force sensitivity to their relative position, particularly in the flange transition area.

Tab. 3 Overview of changes in value of guiding wheel force Y, contact point in flange transition; $Q = 100\ \mathrm{kN}$, $v_{\mathrm{ref}} = 10\ \mathrm{m\ s^{-1}}$, $s_{\mathrm{x}} = 0$, calculated with CONTACT

Lateral offset [mm]	Guiding force Y [kN]	Angle of attack [mrad]	Guiding force Y [kN]
0,0	43.8	0.0	43.8
0,1	82.4	10.0	37.6
0,2	131.6	20.0	91.2
0,3	161.3	30.0	131.1
0,4	176.8	40.0	131.4

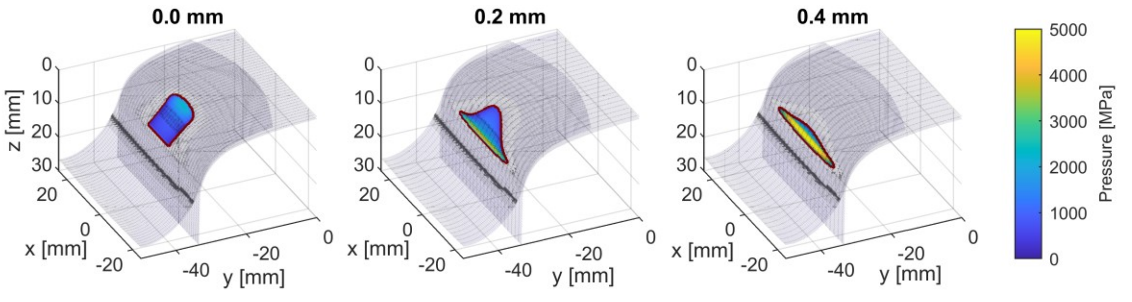

Fig. 7 Changes in contact patch shape and normal pressure distribution with lateral movement, CONTACT

Measurements Designs

The first part of the design deals with lateral displacement and angle of attack. Both measurements will be performed using displacement sensors. The principle of the measurement is shown in Fig. 8. Each roller is equipped with a pair of displacement sensors that measure the distance of the two points on a roller's rim. These measured points are located on a known distance from axis of rotation – the measuring base (L_r on the rail roller, L_w on the wheel roller). This configuration enables measurement of the lateral displacement (y_r for the rail roller and y_w for the wheel roller – Eqn. (9)) and the yaw angle (α_r for the rail roller and α_w for the wheel roller – Eqn. (10)) from tangent. This configuration has following advantages.

- Measurement of all relevant movements close as possible to the contact point (minimising test rig flexibility influence).
- Ability to measure all parasitic movements of the rollers (see Tab. 2)
- Possibility of sensors calibration and zeroing against a common base.
- Easier installation and alignment using a single jig.

$$y_\mathrm{r} = \frac{y_1 + y_2}{2};\; y_\mathrm{w} = \frac{y_3 + y_4}{2} \Rightarrow y = y_\mathrm{r} - y_\mathrm{w} \tag{9}$$

$$\tan \alpha_\mathrm{r} = \frac{y_2 - y_1}{2L_\mathrm{r}};\; \tan \alpha_\mathrm{w} = \frac{y_4 - y_3}{2L_\mathrm{w}} \Rightarrow \alpha = \alpha_\mathrm{w} - \alpha_\mathrm{r} \tag{10}$$

The basic design parameters of the measuring system are listed in Tab. 4. From these, the most important criterion for sensor selection is the minimum required measuring range $y_\mathrm{n,min}$ (for $n = 1; 2; 3; 4$).

Tab. 4 Basic design parameters of the measuring system

Parameter	**Abbr.**	**Value – rail roller**	**Value – wheel roller**
Measuring base	L_r, L_w	200 mm	200 mm
Maximum yaw angle	$\alpha_\mathrm{r,max}$, $\alpha_\mathrm{w,max}$	$\pm 1°$	$\pm 5°$
Maximum lateral displacement	$y_\mathrm{r,max}$, $y_\mathrm{w,max}$	86 mm	± 1 mm
Minimum required measuring range of the sensor	$y_\mathrm{n,min}$	90 mm	50 mm

Since the measuring system must determine the distance between moving and stationary parts, only optical measurement methods can be used. Therefore, four *Micro-Epsilon optoNCDT 1302* sensors with a 100 mm measuring range were selected (specification [8]). The design in CAD model is in Fig. 9.

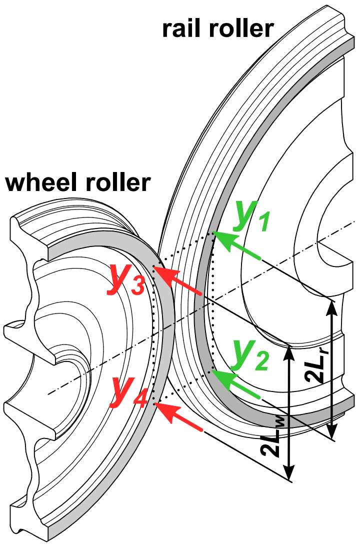

Fig. 8 Principle of measurement

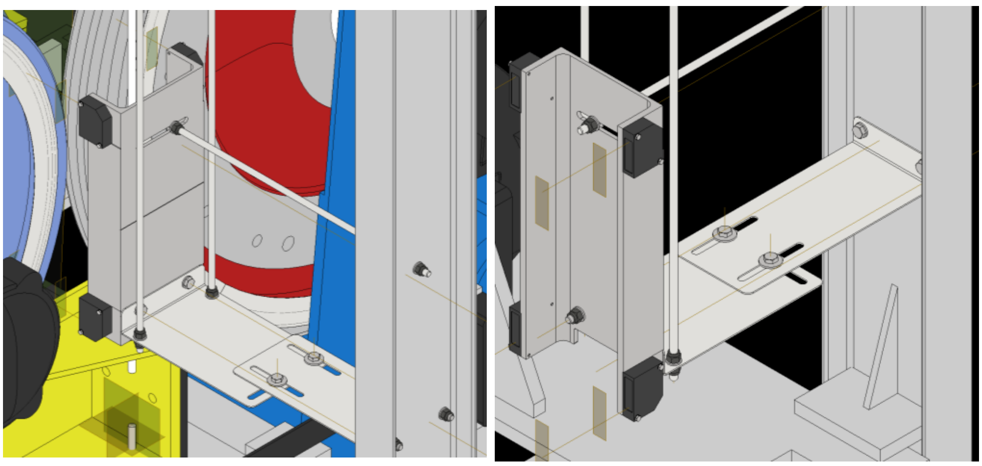

Fig. 9 Mechanical design of the measuring system in CAD

The final part of the measurement system addresses the angle ψ on the wheel roller. For this purpose, we presume to measure deflection on end of the wheel roller's frame. To evaluate this, the deflection at the end of the wheel roller frame will be measured. Although this parasitic movement may be negligible, this measurement aims to determine its significance. Another *Micro-Epsilon optoNCDT 1302* sensor will be used. The angle will be evaluated from the measured deflection and lateral movement y_w with same the same principle described with Eqn. (10).

5 CONCLUSION

The continuation of experiments aimed at determining the influence of spin on the distribution of forces between the wheel and rail requires precise measurements. In this paper, we proposed improvements to the measuring system installed on the RWTR, which will be used in the planned experiments. These improvements enhance the measuring capabilities related to the relative position of the rollers.

First, we discussed the theory of adhesion and the resulting possibilities for measuring the influence of spin. Based on this analysis, we identified the set of quantities required to measure and evaluate the experiments. Although the RWTR is equipped with an extensive measuring system, the relative position of the rollers—comprising the lateral displacement and the angle of attack—is not measured with sufficient precision. Numerical calculations of the contact conditions indicate the required level of precision. To meet these requirements, an integrated measuring system for determining the relative position was designed.

Future work will focus on verifying the adequacy of this design. The basic principle of this verification will be based on a comparison with numerical calculations of the contact conditions.

The research was supported by the University of Pardubice, project of the Student Grant Competition SGS_2025_008 “Recent aspects in the field of transport means and infrastructure solved at the FTE”.

◆◆

References

[1] KALKER, J. J. *Three-dimensional elastic bodies in rolling contact*. Dordrecht: Springer Netherlands, 1990. ISBN 978-90-481-4066-4.

[2] PULDA, J., CULEK, B., VOLTR, P. Experimental proof of spin influence on rail-wheel contact forces: State of present knowledge (in Czech). In: *Súčasné problémy v koľajových vozidlách – PRORAIL 2023: XXVI. medzinárodná konferencia, zborník prednášok*, *diel II*. Žilina: VTS pri ŽU v Žiline, 2023, pp. 175–182. ISBN 978-80-89276-62-2.

[3] CULEK, B., MALINSKÝ, J., CULEK, B. jr. Výzkum na testovacím zařízení železničních kol. *Nová železniční technika.* Roč. 2007, č. 2, pp. 20–22. ISSN 1210-3942.

[4] HARTWIG, P. *Konstruktive Anpassung des Eisenbahnradprüfstandes der Universität Pardubice an die Messung von Adhäsionserscheinungen*. Diplomarbeit. Dresden: Hochschule für Technik und Wirtschaft Dresden, 2006.

[5] VOLTR, P. *Konstrukční námět zabudování dynamické brzdy do Testovacího zařízení železničních kol*. Report no. 01/12. Project no. TA02030776 Technique for measuring the force effects in the wheel-rail contact. Pardubice: University of Pardubice, Faculty of Transport Engineering, 2012.

[6] CULEK, B. *Experimenty na Testovacím zařízení železničních kol*. Report no. 01/2015. Project no. TA02030776 Technique for measuring the force effects in the wheel-rail contact. Pardubice: University of Pardubice, Faculty of Transport Engineering, 2015.

[7] BRICKLE, B. V. *The steady state forces and moments on a railway wheelset including flange contact conditions*. A Doctoral Thesis. Loughborough: Loughborough University of Technology, 1973. Available from: https://hdl.handle.net/2134/16979. [cited 2025-06-06]

[8] *optoNCDT 1302: Laser Triangulation Displacement Sensors*. Ortenburg: Micro-Epsilon.

[9] VOLLEBREGT, E. Detailed wheel/rail geometry processing using the planar contact approach. *Vehicle System Dynamics*. Vol. 60 (2020), no. 4, pp. 1253–1291. ISSN 0042-3114.

[10] VOLLEBREGT, E. Detailed wheel/rail geometry processing with the conformal contact approach. *Multibody System Dynamics*. Vol. 52 (2020), no. 2, pp. 135–167. ISSN 1384-5640.

Received / zasláno: 23. 06. 2025, accepted / přijato: 15. 07. 2025, published / publikováno: 17. 09. 2025.

The paper was reviewed by / Příspěvek recenzovali: Ing. Jan Kalivoda, Ph.D. (Czech Technical University in Prague, Faculty of Mechanical Engineering), prof. Dr. Ing. habil. Oldřich Polách.